

**Enhancing collision avoidance in mixed waterborne transport
Human-mimic navigation and decision-making by autonomous vessels**

Song, Rongxin; Papadimitriou, Eleonora; Negenborn, Rudy R.; van Gelder, Pieter

DOI

[10.1016/j.oceaneng.2025.120443](https://doi.org/10.1016/j.oceaneng.2025.120443)

Publication date

2025

Document Version

Final published version

Published in

Ocean Engineering

Citation (APA)

Song, R., Papadimitriou, E., Negenborn, R. R., & van Gelder, P. (2025). Enhancing collision avoidance in mixed waterborne transport: Human-mimic navigation and decision-making by autonomous vessels. *Ocean Engineering*, 322, Article 120443. <https://doi.org/10.1016/j.oceaneng.2025.120443>

Important note

To cite this publication, please use the final published version (if applicable).
Please check the document version above.

Copyright

Other than for strictly personal use, it is not permitted to download, forward or distribute the text or part of it, without the consent of the author(s) and/or copyright holder(s), unless the work is under an open content license such as Creative Commons.

Takedown policy

Please contact us and provide details if you believe this document breaches copyrights.
We will remove access to the work immediately and investigate your claim.



Research paper

Enhancing collision avoidance in mixed waterborne transport: Human-mimic navigation and decision-making by autonomous vessels

Rongxin Song^{a,*}, Eleonora Papadimitriou^a, Rudy R. Negenborn^b, Pieter van Gelder^a

^a Safety and Security Science Group, Delft University of Technology, the Netherlands

^b Department of Maritime and Transport Technology, Delft University of Technology, the Netherlands

ARTICLE INFO

Keywords:

Collision avoidance
 Navigational preferences
 Long short-term memory (LSTM)-Autoencoder
 Multi-task learning sequence-to-sequence attention LSTM
 Predictive decision-making
 K-means clustering

ABSTRACT

Collision avoidance in maritime navigation, particularly between autonomous and conventional vessels, involves iterative and dynamic processes. Traditional path planning models often neglect the behaviours of surrounding vessels, while path predictive models tend to ignore ship interaction features essential in collision scenarios. This study proposes a decision-making framework for collision avoidance, particularly focused on the interaction between autonomous and conventional vessels. The framework integrates a human-preference-aware navigational trajectory prediction model into the collision avoidance process, enhancing the decision-making capabilities in dynamic and interactive environments. We first model human-controlled ship navigational preferences using a Long Short-Term Memory (LSTM) autoencoder combined with K-means clustering, by extracting key preferences from ship pairs identified through AIS data. These preferences, which reflect strategic trajectory adjustments in response to collision risks, are then incorporated into trajectory prediction using a Multi-Task Learning Sequence-to-Sequence (seq2seq) attention LSTM model. The predicted trajectories provide a basis for the decision-making framework, including a local path planner and a trajectory tracking controller, designed to dynamically adjust the predicted reference path for collision-free navigation and ensure its accurate tracking. The framework was validated using AIS data from the port of Rotterdam, identifying four distinct navigational preferences by combining an LSTM-autoencoder and clustering techniques and demonstrating improved prediction accuracy compared to other existing models. Simulation tests demonstrate that the framework utilises the predicted trajectories to inform decision-making, ensuring accurate path tracking while dynamically addressing collision risks for autonomous ships. By providing preference-aware and adaptive reference trajectories, the framework reduces the likelihood of MASS trajectory misinterpretation by conventional ships, thereby supporting proactive collision avoidance in mixed waterborne transport environments.

1. Background and objectives

With the advent of the Maritime Autonomous Surface Ships (MASS), there is an opportunity to enhance navigational safety and efficiency (Song et al.). MASS, capable of operating with varying degrees of autonomy, aims to reduce human error and operational costs. However, integrating MASS with conventional manned ships in mixed waterborne environments presents new challenges, particularly in collision avoidance (Huang et al., 2020).

Current collision avoidance methods primarily focus on algorithmic capabilities such as deterministic path planning and optimisation algorithms that prioritise minimising travel time or fuel consumption (Akdağ et al., 2024) while maintaining navigational safety (Shu et al., 2023) and

complying with International Regulations for the Prevention of Collisions at Sea (COLREGS). These methods often use pre-defined rules or optimisation criteria to generate collision-free paths for vessels. However, most of these models typically overlook the dynamic and interactive behaviours of surrounding vessels. For instance, human-operated ships tend to adjust their manoeuvres based on the perceived intentions of neighbouring vessels, a behaviour that is not accounted for in many algorithmic models. This oversight can lead to less accurate and interpretable predictions in real-time collision scenarios. Additionally, existing models often fail to incorporate dynamic manoeuvres such as high speed with a small starboard side turn and a minor acceleration. These navigational behaviours, typically exhibited by human operators to ensure efficient and safe navigation, highlight the importance of

* Corresponding author.

E-mail address: r.song@tudelft.nl (R. Song).

<https://doi.org/10.1016/j.oceaneng.2025.120443>

Received 6 November 2024; Received in revised form 3 January 2025; Accepted 18 January 2025

Available online 30 January 2025

0029-8018/© 2025 The Authors. Published by Elsevier Ltd. This is an open access article under the CC BY license (<http://creativecommons.org/licenses/by/4.0/>).

mimicking human-like decision-making behaviours, which will be referred to in the present research as ‘**human preferences**’. By incorporating such human-mimic behaviours, future models could better capture human operators’ adaptive and flexible nature, improving MASS’s accuracy and safety in a mixed waterborne environment.

1.1. Problem statement

Given the limitations of current models, there is a need for enhanced predictive models that can integrate navigational preferences in trajectory prediction and, eventually, decision-making algorithms. This requires a comprehensive decision-making framework that not only predicts trajectories based on navigational preferences but also integrates these predictions into collision avoidance strategies.

Automatic Identification System (AIS) data is instrumental in this recognition process, providing real-time information crucial for identifying potential collision scenarios and the consecutive evasive manoeuvres reflecting human navigational preferences. The dynamics of vessel interactions and the decision-making processes between conventional ships performing collision avoidance can be captured by analysing and modelling AIS data through machine learning methods.

1.2. Motivation

This study is motivated by the need to bridge an important gap in implicit communication between autonomous collision avoidance systems and conventional vessels, aiming to develop a framework for MASS to understand the navigational intentions of neighbouring ships and predict their movements for further decision-making in the collision avoidance phase. By incorporating human-mimic behaviours, MASS can more effectively interact with human-operated ships. More specifically, this study seeks to address the following key research questions.

1. How can AIS data be utilised to extract the navigational preferences of conventional vessels for collision avoidance?
2. How can past vessels’ trajectories be used to develop a real-time movement prediction model with improved accuracy and interpretability based on human navigational preferences?
3. How does the prediction result support the interactive collision avoidance of MASS in a mixed waterborne environment?

To answer these questions, this study will extract navigational preferences from AIS data to gain insights about ship manoeuvring dynamics in collision avoidance scenarios based on an LSTM-autoencoder with the K-means clustering algorithm. Moreover, the study will develop a Multi-Task Learning (MTL) Sequence-to-Sequence LSTM model with an attention mechanism, abbreviated as MTL-Seq2Seq-LSTM-Att, to predict future trajectories of both the own and neighbouring ships, by integrating the navigational preferences extracted from AIS data into the model as specific tasks. Finally, in this paper, we extend the decision-making framework proposed in a previous study by (Song et al. 2022, 2024) by taking into account the preference-aware trajectory generated by the predictive model to make a safer, more efficient, and more proactive interaction in a mixed waterborne transport environment.

This paper is structured as follows: Section 2 reviews existing methodologies and highlights the gaps in current approaches to maritime collision avoidance. Section 3 details the methodology of the predictive model and the decision-making framework developed in this study. Section 4 describes the experimental setup, evaluates the models’ performance through various metrics, and validates the decision-making framework through simulation. Sections 5 and 6 discuss the proposed

methodology, summarise the findings and implications of this research, and suggest directions for future research, respectively.

2. Recent work

In the crucial domain of maritime navigation, the detection of collision conflicts has evolved greatly, incorporating state-of-the-art big data analytics, predictive modelling, and computational techniques to improve the safety navigation of MASS, by enhancing MASS’s situational awareness, predictive capabilities, and further decision-making.

2.1. Collision conflict detection

A study by (Chen et al., 2018) utilises AIS data to analyse collision risks dynamically by using a velocity obstacle approach, highlighting the necessity of timely and accurate risk assessments. Similarly, research conducted by (Liu et al., 2019) applied spatial clustering and analytical methods to manage collision risks. Additionally, an investigation by (Xin et al., 2021) estimates collision risk among multiple vessels and leverages spatiotemporal patterns and a two-stage Monte Carlo simulation algorithm, thereby enhancing prediction accuracy and efficiency for potential collision scenarios. Research conducted by (Liu et al., 2021) and (Rong et al., 2022) focused on identifying high-collision potential areas and analysing ships’ reactions in near-collision scenarios. Additionally, the studies by (Zhang et al., 2021; Gil, 2021) employed geometric and operational parameter analyses to aid proactive collision avoidance. These studies contributed to improved targeted interventions and collision conflict detection capabilities.

The concept of ship domain and the Collision Threat parameter area method have been extensively studied by (Szlapczynski and Krata, 2018) and (Szlapczynski and Szlapczynska, 2021). These approaches integrate environmental factors and ship stability considerations, supporting navigators executing informed collision avoidance manoeuvres.

Studies by (Westrenen et al., 2020) and (Huang et al., 2018) have examined the impact of maritime traffic complexity and the application of Velocity Obstacle algorithms on collision conflict detection, respectively. By addressing the limitations of traditional techniques and introducing methods that consider non-linear and time-dependent ship trajectories, these studies offer more realistic solutions for collision avoidance and reducing false alarms. Furthermore, the application of knowledge graphs has been demonstrated to uncover correlations between critical factors in ship collision scenarios (Gan et al., 2023), enabling the identification of causal relationships and supporting decision-making in collision avoidance scenarios.

These efforts highlight the evolution of maritime collision avoidance strategies, showcasing innovative methods that integrate dynamic risk assessments, spatial clustering, and simulation algorithms to improve safety and decision-making in complex maritime environments. While these approaches are well-established, our study presents a method aimed at extracting trajectory conflict pairs from AIS data. By focusing on identifying vessel trajectory pairs at risk of collision and defining relevant navigational parameters, this method provides a tailored approach for detecting potential collisions for further navigational preferences extraction.

2.2. Intention identification

In maritime navigation, the key task of predicting vessel intentions to enhance safety and prevent collisions has seen great advancements through innovative methodologies.

Research by (Murray and Perera, 2018) introduced trajectory

prediction for autonomous vessels, emphasising the need for ships to anticipate neighbouring movements for collision avoidance. This foundational work underscores the importance of predictive analytics in autonomous maritime navigation. Expanding on predictive approaches, the investigation by (Du et al., 2020) focused on situational awareness by estimating intentions of give-way and stand-on ships, enabling vessels to make informed decisions and enhance proactive safety measures.

The study by (L. Huang et al., 2020) applied semantic analysis and topic modelling borrowed from Natural Language Processing to maritime trajectory data. By identifying mobility patterns, this work contributed to route discovery (Huang et al., 2024) and anomaly detection. The study by (Szlapczynski et al., 2018) utilised the ship domain concept to precisely predict time avoidance manoeuvres and improve decision-making accuracy in critical scenarios. Additionally, environmental factors that influence vessel behavior are important to be considered in intention identification. For example, the spatio-temporal correlation between tides and ship movements in estuarine ports (Shu et al., 2024).

In leveraging AIS, the research presented by (Zhang et al., 2023) developed a knowledge-based decision support system using AIS data to guide ship collision avoidance, including encounter identification, behaviour extraction, and scenario matching to generate safe navigation paths. Additionally, research presented by (Zhang et al., 2020) introduced a dynamic system for multi-ship collision avoidance, focusing on predicting vessel intentions through an iterative observation-inference-prediction-decision model.

The approach developed by (L. Chen et al., 2018) investigated the cooperative control of autonomous vessels, particularly in the formation and maintenance of a “vessel train.” This study highlights the significance of coordinated behaviour and communication among vessels to improve navigational safety and respond effectively to dynamic maritime environments.

While existing studies have made much progress in intention identification and enhancing situational awareness, many approaches focus on specific scenarios or utilise methods that may not fully capture the sequential features of time-series navigational data. For example, directly applying clustering techniques to high-dimensional trajectory data may be a challenge due to the complexity and temporal dependencies inherent in such data. This suggests a need for methods that can better account for these temporal dynamics, allowing for a more detailed analysis of vessel intentions during the interaction.

2.3. Trajectory prediction

LSTM networks are increasingly recognised for their effectiveness in sequence prediction, making them particularly well-suited for forecasting vessel trajectories using AIS data. Research has consistently highlighted LSTM’s capability to handle the sequential nature of AIS data, such as the work by (Thind et al., 2022), which focuses on dynamically adapting to the most recent known positions.

Building on the foundational strengths of LSTM, recent research has introduced hybrid models that combine LSTM’s predictive capabilities with other computational techniques to better address the particularities of the maritime environment. For example, the study by (Liu et al., 2022) leveraged the learning capacity of LSTM within an IoT framework to promote smart traffic services, demonstrating high accuracy and robustness in predicting vessel trajectories. Furthermore, the research by (Liu et al., 2023) proposed an interactive vessel trajectory prediction framework, embedding the Quaternion Ship Domain into LS and addressing dynamic interactions between neighbouring vessels. It has

demonstrated better performance than existing methods.

Moreover, integrating LSTM with emerging technologies like graph convolutional networks and context-aware systems underscores a potential trend in maritime traffic management. Research presented by (Gao et al., 2024) utilised an LSTM within a spatiotemporal edge and node attention graph convolutional network for handling multi-ship encounters. Additionally, research by (Zhang et al., 2024) proposed a Dynamic Spatio-Temporal Graph Attention Network incorporating LSTM for short-term motion pattern perception. Additionally, the study conducted by (Wang et al., 2024) introduced a deep attention-aware spatiotemporal graph convolutional network, including an LSTM module for motion feature extraction, improving prediction accuracy in complex sea areas. In addition, the incorporation of contextual information into LSTM models has also been shown to enhance prediction outcomes. The study by (Mehri et al., 2023) designed a context-aware LSTM framework that integrates contextual information such as wind, wave size, and current, showing an improvement in accuracy over standard LSTM approaches.

Additionally, the application of LSTM in conjunction with clustering techniques has proven effective in enhancing situational awareness of autonomous ships and aiding proactive collision avoidance strategies. Research by (Murray and Perera, 2022) implemented clustering techniques combined with LSTM for extracting trajectory segments from historical AIS data. Another study by (Yang et al., 2022) developed a model combining the DBSCAN algorithm and LSTM, which cluster vessel tracks before prediction. The study presented by (Alam et al., 2024) enhanced short-term vessel trajectory prediction by clustering routes and using Random Forest algorithms, demonstrating accuracy improvements for heterogeneous and multi-modal movement patterns.

Seq2seq models have also been introduced into maritime trajectory prediction. A multi-task learning model based on the attentional seq2seq framework was proposed by (Jiang et al., 2024), jointly learning route patterns and future trajectories. The study by (Düz and van Iperen, 2024) employed encoder-decoder architectures for ship trajectory prediction using AIS data and achieved an accurate prediction.

The application of LSTM and its variants in vessel trajectory prediction has demonstrated much progress in accuracy and reliability. By integrating LSTM with clustering techniques, context-aware frameworks, graph convolutional networks, and other models, researchers have developed various methods that address the prediction of ship trajectories. The adaptability of LSTM makes it an essential technology in vessel trajectory prediction.

3. Methodology

3.1. Navigational preference modelling and extraction

This section presents the methodological approach to model human navigational preferences in collision avoidance scenarios. We detail the process from navigational preference definition to collision conflict pairs extraction and preference extraction based on an LSTM-autoencoder.

3.1.1. Definition of navigational preference

Understanding and predicting the relative dynamic relationship between two vessels is crucial in vessel collision avoidance decision-making, especially in relatively open waters, such as the open sea or port areas. In these environments, geographical constraints on vessel movement are minimal, and collision avoidance decisions primarily depend on relative motion parameters. This study examines navigation preferences in these scenarios with minimal geographical constraints.

Table 1
Features selected for preference identification in collision avoidance scenarios.

Variables	Explanation of selection
SOG1, SOG2	Indicate the rates at which two vessels are approaching or moving away from each other.
ROT1, ROT2	Indicate the rates at which two vessels change their headings.
ACC1, ACC2	Indicate the rates at which two vessels change their speeds.
α, ϕ	Uniquely determine the encounter situation and navigational priority between vessels.
DCPA, TCPA	Denotes the minimum distance and time until the vessels reach the closest point of approach.

Definition. Human Navigational preference refers to the decision-making tendencies and behavioural patterns exhibited by a vessel within the relative motion space based on the dynamic relationship between two vessels. This preference is generally independent of absolute position and heading, reflecting the vessel's operators' choices in collision avoidance through relative motion.

Symbols:

SOG1, SOG2: the speeds over ground of the own ship and the neighbouring ship, respectively;

ROT1, ROT2: Rates of turn of the own ship and the neighbouring ship, respectively;

ACC1, ACC2: Acceleration of the own ship and the neighbouring ship, respectively;

α, ϕ : Relative bearing and encounter angle;

DCPA: Distance closest point of approach;

TCPA: Time closest point of approach.

The features presented in Table 1 for modelling navigational preferences are selected to identify the preference required for collision avoidance.

3.1.2. Collision conflict pairs extraction

In order to collect information from ship movement for further investigation, we propose an algorithm to extract collision conflict pairs from raw AIS data (see Algorithm 1). The algorithm focuses on identifying instances where vessels come within a pre-defined proximity threshold, thereby filtering out irrelevant data and concentrating on encounters that may call for navigational adjustments. This procedure ensures that only noticeable events are analysed for potential collision risks. This algorithm employs geohashing to facilitate quick spatial comparisons, ensuring the efficiency of detecting potential collisions.

The detection process begins with preprocessing raw AIS data to ensure high-quality and reliable input. This includes interpolating missing data, detecting and removing outliers, and sampling the data for efficient processing. Trajectories are segmented based on a time threshold Δt , set at 3 min, to differentiate continuous from discontinuous vessel movements. Geohashes are then calculated for each segment, converting geographic coordinates into compact alphanumeric strings. This encoding method allows for rapid spatial comparisons within the same geohash bucket (Moussalli et al., 2015), identifying potential collision pairs based on spatial proximity and temporal overlap.

Finally, the dataset is prepared and indexed by $\{(mmsi_{m1}, seg_{s1}), (mmsi_{m2}, seg_{s2})\}$ of potentially colliding ship pairs. Here, $mmsi_{m1}$ represents the MMSI number (Maritime Mobile Service Identity) of the first ship in the pair, and seg_{s1} refers to the s_1 -th trajectory segment of that ship. Similarly, $mmsi_{m2}$ and seg_{s2} correspond to the MMSI number and trajectory segment of the second ship. Additionally, critical navigational parameters, such as DCPA, TCPA, α, ϕ , Encountered situations (ES), and navigational priorities (NP), are calculated for each identified potential collision pair. This data provides a foundation for further data-driven preferences investigation.

Algorithm 1. Potential Collision Conflict Pairs Detection And Contextual Info Annotation

Algorithm 1: Potential Collision Conflict Pairs Detection and Contextual Info Annotation

- 1 **Input:** Raw AIS data
- 2 **Output:** List of potential collision pairs
- 3 **Step 1: Preprocess the AIS data**
- 4 Apply interpolation, outlier detection, and sampling on AIS data.
- 5 **Step 2: Trajectory Segmentation**
- 6 **foreach** $MMSI\ mmsi_m$ **in** AIS data **do**
- 7 Segment trajectories based on time intervals exceeding Δt (e.g., 3 minutes);
- 8 Store segmented trajectories: $Tra_{mmsi(m,s)} \leftarrow (mmsi_m, seg_s)$;
- 9 **Step 3: Compute Geohashes for Trajectory Segments**
- 10 Initialise dictionary GeohashBuckets;
- 11 **foreach** $(mmsi_m, seg_s)$ **do**
- 12 Calculate geohashes for each position (latitude, longitude) in $(mmsi_m, seg_s)$;
- 13 Store $(mmsi_m, seg_s)$ in GeohashBuckets under its geohash;
- 14 **Step 4: Identify Potential Collision Pairs**
- 15 Initialise set PotentialCollisions;
- 16 **foreach** $bucket$ **in** GeohashBuckets **do**
- 17 **if** $length\ of\ bucket > 1$ **then**
- 18 **foreach** $unique\ pairs\ \{(mmsi_{m1}, seg_{s1}), (mmsi_{m2}, seg_{s2})\}$ **with**
 $m_1 \neq m_2$ **in** bucket **do**
- 19 **if** $time\ windows\ of\ \{(mmsi_{m1}, seg_{s1}), (mmsi_{m2}, seg_{s2})\}$
 $overlap$ **then**
- 20 Add $\{(mmsi_{m1}, seg_{s1}), (mmsi_{m2}, seg_{s2})\}$ to
PotentialCollisions;
- 21 **Step 5: Calculate Navigational Parameters**
- 22 **foreach** $pair$ **in** PotentialCollisions **do**
- 23 Compute DCPA, TCPA, Encounter angle, and Relative bearing;
- 24 Identify encounter scenarios and navigational priorities;
- 25 **Results:**
- 26 Index: $\{(mmsi_{m1}, seg_{s1}), (mmsi_{m2}, seg_{s2})\}$;
- 27 Manoeuvring Info: $\{SOG_1, ROT_1, ACC_1, SOG_2, ROT_2, ACC_2, \alpha, \phi\}$;
- 28 Contextual Info: $\{DCPA, TCPA, ES, NP_1, NP_2\}$;
- 29 **return** List of potential collision pairs with contextual information;

3.1.3. LSTM-autoencoder for preference extraction

To capture and represent navigational preferences, we employed an LSTM-based autoencoder architecture, as illustrated in Fig. 1. The process begins with an input sequence x , which consists of multiple interaction features (SOG1, SOG2, ACC1, ACC2, ROT1, ROT2, DCPA, TCPA, α and ϕ) that characterise the dynamic interaction between vessels over time.

LSTM-Encoder (f): The LSTM-Encoder, represented by the function f , processes this input sequence x to generate a compressed low-dimensional representation known as the **Representation Vector**. This vector refers to the latent space representation of the original feature sequence, serving as a compact representation of the vessel's interactive actions.

LSTM-Decoder (g): The latent vector, that is, the representation vector, is then fed into the LSTM-Decoder, denoted by the function g , which attempts to reconstruct the original interaction sequence \tilde{x} . The objective of this autoencoder is to minimise the difference between the original input x and the reconstructed output \tilde{x} , ensuring that the representation vector accurately captures the relevant features of the interaction sequence. The loss function of the autoencoder is represented by:

$$Loss_autoencoder = \frac{1}{N} \sum_{i=1}^N \|x_i - \tilde{x}_i\|^2 \quad (1)$$

Subsequent to the autoencoding process, the **Representation Vector** is subjected to K-means clustering for preference extraction. This

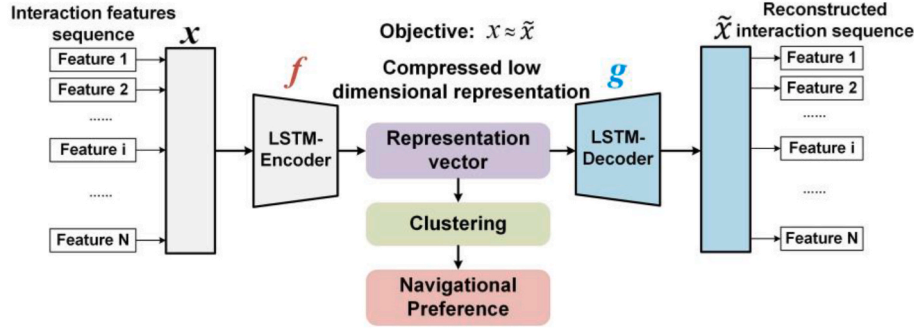


Fig. 1. The scheme of LSTM-Autoencoder for compressing sequence manoeuvres data.

step groups similar vectors together, identifying distinct navigational preferences. These preferences are derived from patterns within the interaction sequences and provide valuable insights into the types of interactive manoeuvres in collision avoidance scenarios.

3.2. Preference-based trajectory prediction

3.2.1. Movement predictor-MTL-Seq2seq-LSTM-Att

The movement predictor proposed for trajectory prediction, that is, a multi-task learning Sequence-to-Sequence LSTM model, enhanced with the Luong attention mechanism (Luong et al., 2015), which aligns and weighs the importance of different input sequence elements, is employed to predict vessels' future movement in collision avoidance scenarios. An LSTM classifier is employed to predict the preference based on the same features as the input features of the LSTM-autoencoder. Furthermore, the navigational preferences serve as the specific tasks to supervise the predictive process, ensuring the prediction accuracy and stability.

The model consists of the following elements, as illustrated in Fig. 2.

(1) Encoder The encoder utilises an LSTM network to process a historical data sequence over a defined time window as the input, including the positions of both the own and the neighbouring ships, the encountered scenario, and navigational priority. The LSTM then generate a series of hidden states that capture temporal dependencies and contextual features of vessel interactions. These representations are essential for the decoder to generate context-aware future trajectories. The mathematical representation of the encoder is given by:

$$(\mathbf{h}_t^{enc}, \mathbf{c}_t^{enc}) = \text{LSTM}(x_t, \mathbf{h}_{t-1}^{enc}, \mathbf{c}_{t-1}^{enc}), (1 \leq t \leq T_s) \quad (2)$$

Where x_t is the input feature vector at time t , T_s refers to the length of the input sequence, \mathbf{h}_t^{enc} and \mathbf{c}_t^{enc} are the hidden and the cell states of the LSTM at time t . \mathbf{h}_{t-1}^{enc} and \mathbf{c}_{t-1}^{enc} represent the hidden and cell states from the previous time step, respectively.

(2) Classifier

The preference is recognised by an LSTM classifier, which receives the same features as the LSTM-autoencoder with the time length of T_s to predict the preference. The representation is given by:

$$y_{\text{pref}} = \text{softmax}(\mathbf{W}_{\text{pref}} \mathbf{h}_{T_s}^{enc} + \mathbf{b}_{\text{pref}}) \quad (3)$$

where y_{pref} represents the navigational preference class of prediction, \mathbf{W}_{pref} , \mathbf{b}_{pref} refer to the weights and bias vectors, respectively.

(3) Task-specific decoder The preference predicted by the classifier is then transmitted into the MTL-Seq2Seq-LSTM-Att model, where the preference is taken as the specific task to decode the input sequences to ensure the alignment between realistic navigational strategies.

$$\mathbf{h}_{t+1}^{task}, \mathbf{c}_{t+1}^{task} = \text{LSTM}(\mathbf{y}_t^{task}, \mathbf{h}_t^{task}, \mathbf{c}_t^{task}) \quad (4)$$

here \mathbf{y}_t^{task} is the input to the decoder at time step t , and \mathbf{h}_t^{task} and \mathbf{c}_t^{task} are the hidden state and cell state of the decoder, respectively.

(4) Attention mechanism

The Luong attention is employed in our model to enhance the relevance and precision of the generated sequences. At each time step t , the decoder utilises a task-oriented attention mechanism to weigh the encoder outputs, producing the corresponding context vector \mathbf{c}_t . This process aligns the decoders' focus with the most relevant features of the input sequence, thereby ensuring that subsequent interactive manoeuvres can be captured based on the ship trajectories over a given timeframe.

$$\alpha_t(s) = \text{softmax}(\text{score}(\mathbf{h}_t^{task}, \bar{\mathbf{h}}_s)) = \frac{\exp(\text{score}(\mathbf{h}_t^{task}, \bar{\mathbf{h}}_s))}{\sum_s \exp(\text{score}(\mathbf{h}_t^{task}, \bar{\mathbf{h}}_s))} \quad (5)$$

$$\text{score}(\mathbf{h}_t^{task}, \bar{\mathbf{h}}_s) = \mathbf{h}_t^{taskT} \mathbf{W}_a \bar{\mathbf{h}}_s \quad (6)$$

$$\mathbf{c}_t = \sum_s \alpha_t(s) \bullet \bar{\mathbf{h}}_s \quad (7)$$

where $\alpha_t(s)$ refers to the attention weight for encoder state s at time t , $\bar{\mathbf{h}}_s$

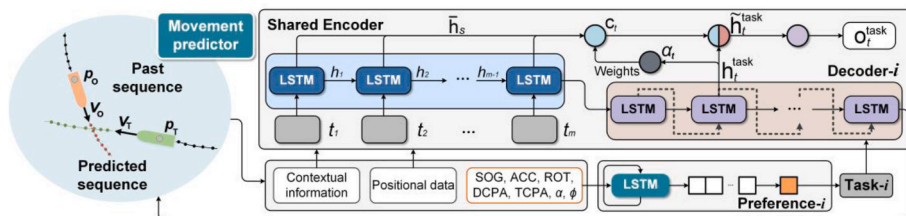


Fig. 2. The diagram of preference-based movement predictor for trajectory prediction.

represents each encoder's hidden state, \mathbf{h}_t^{task} is the current decoder hidden state, and the score $(\mathbf{h}_t^{task}, \bar{\mathbf{h}}_s)$ is the score function that measures the match between the decoder state \mathbf{h}_t^{task} and the encoder state $\bar{\mathbf{h}}_s$ through the trainable weight matrix \mathbf{W}_a .

The attentional state of the decoder $\tilde{\mathbf{h}}_t$ is updated through:

$$\tilde{\mathbf{h}}_t = \tanh(\mathbf{W}_c \bullet \text{concat}(c_t; h'_t)) = \tanh(\mathbf{W}_c \bullet [c_t; h'_t])$$

with \mathbf{W}_c being a trainable parameter matrix with the dimension of $[n_h \times 2n_h]$ transforms the context vector c_t and decoder hidden state h'_t into an attentional hidden state.

(5) Output layer

$$(\mathbf{h}_t^{enc}, \mathbf{c}_t^{enc}) = \text{LSTM}(x_t, \mathbf{h}_{t-1}^{enc}, \mathbf{c}_{t-1}^{enc}), (1 \leq t \leq T_s) \quad (8)$$

$$\mathbf{o}_t^{task} = \mathbf{W}_{out}^{task} [\mathbf{c}_t; \mathbf{h}_t^{task}] + \mathbf{b}_{out}^{task} \quad (9)$$

where \mathbf{W}_{out}^{task} is the weight matrix for the linear transformation of the specific task, \mathbf{b}_{out}^{task} is the bias vector for a specific task.

3.2.2. Decision-making framework for collision avoidance

In order to ensure safe and efficient navigation in mixed waterborne transport environments, this study proposes a decision-making framework for MASS by integrating the predictive model above with previous work. This section details how our framework employs the predictive model introduced in section 3.3.2 and integrates it with Knowledge Maps (KM) developed in our previous work (Song et al., 2022) and Local Planner Dynamic Window Approach (DWA) proposed in a subsequent study (Song et al., 2024). The framework is illustrated in Fig. 3.

The core components and their interactions are outlined as follows.

- (1) **Knowledge Maps (KM):** The module processes real-time environmental data and historical movement trajectories to support other modules. It provides inputs for the Movement Predictor and decision-making algorithms by transferring relevant requirements to executable actions. This module updates continuously, ensuring the system operates with accurate context-aware information, as detailed in (Song et al., 2022).
- (2) **Movement Predictor:** When surrounding vessels are detected, this module employs the prediction model described in Section 3.3.2 to forecast the trajectories of both the own and neighbouring ships. Based on these predicted trajectories, the module constructs the reference path, a human-preferred evasive route for the own ship in the current collision avoidance scenario. This reference path ensures that the MASS behaves in a manner that is predictable and comprehensible to human operators on nearby

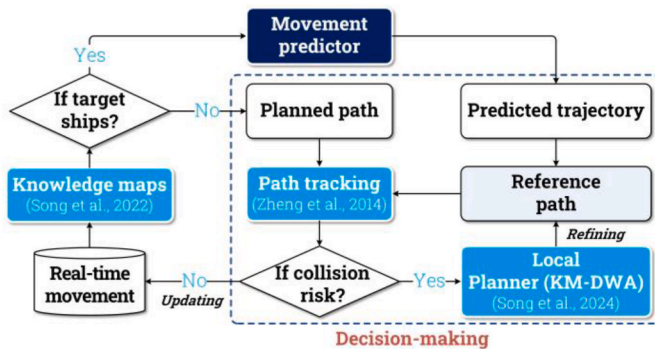


Fig. 3. The diagram of the decision-making framework based on trajectory prediction.

vessels, reducing the potential for misinterpretation of the MASS's intentions.

- (3) **Risk Assessment:** Risk Assessment evaluates potential collision risks based on pre-defined safety thresholds, such as DCPA and TCPA, considering the manoeuvrability of the own ship. As shown in the bottom-right part of Fig. 3, if any risk is detected, the local planner (KM-DWA) proposed by (Song et al., 2024) implements the local planning task for refining the reference path. Conversely, if no risks are detected, the vessel continues to follow the reference path. This mechanism ensures the navigational safety of MASS in dynamic environments.
- (4) **Local Planner - KM-DWA:** If a collision risk is detected, the Local Planner module is activated. Using the KM-DWA algorithm, this module refines the reference path by making localised adjustments to mitigate collision risks. This refinement does not involve generating a completely new path; instead, it focuses on fine-tuning the existing reference path to adhere closely to human navigational preferences. The updated reference path ensures that the MASS avoids collisions while navigating in a manner that remains predictable and understandable to human operators on surrounding vessels.
- (5) **Path Tracking:** This module ensures accurate execution of the reference path. A non-linear model predictive control (MPC) algorithm proposed by (Zheng et al., 2014) is employed in this decision-making framework to track the reference path.

3.3. Model parameters determination

3.3.1. LSTM-autoencoder

- (1) **Model Structure:** The LSTM-Autoencoder consists of an encoder and a decoder, each comprising two LSTM layers. The encoder compresses the input sequence with a hidden dimension of 128 into a lower-dimensional latent representation with a dimension of 64, while the decoder reconstructs the sequence from this compressed form.
- (2) **Training:** The training process utilises the AdamW optimiser with a learning rate of 0.001, balancing effective learning and regularisation. Additionally, a ReduceLROnPlateau scheduler is applied, reducing the learning rate when the model's performance plateaus and helping to fine-tune the model over training epochs.

3.3.2. MTL-Seq2Seq-LSTM-Att model

3.3.2.1. (1) **Model Structure.** The encoder and decoder consist of two LSTM layers and a hidden dimension of 128. The encoder processes the input sequence to capture temporal patterns and compresses this information into a context vector, while the decoder outputs the corresponding future trajectories based on the given sequence.

A custom loss function was implemented to handle the multi-output nature of the task, particularly focusing on the accuracy of predicted trajectories for both the own vessel and the neighbouring vessel.

3.3.2.3. (3) **Runtime performance.** This module operates as a real-time part of the decision-making framework, predicting vessel trajectories in the next few minutes. Runtime performance is critical for ensuring the system's feasibility in real-time scenarios, which is evaluated by measuring average runtime across multiple trials with an 11th Gen Intel (R) Core(TM) i7-1185G7 @ 3.00 GHz processor.

3.3.3. Evaluation metrics

Several metrics were used to assess the model's performance.

- 1) Root Mean Squared Error (RMSE): RMSE was calculated to measure the average magnitude of reconstruction errors, with a lower RMSE indicating better model performance.

$$RMSE = \sqrt{\frac{1}{n} \sum_{i=1}^n (y_i - \hat{y}_i)^2}$$

where, y_i represents the actual value, \hat{y}_i represents the predicted value, and n is the number of data points.

- 2) Mean Squared Error (MSE): MSE was calculated to measure the average magnitude of the squared reconstruction errors, with a lower MSE indicating better model performance.

$$MSE = \frac{1}{n} \sum_{i=1}^n (y_i - \hat{y}_i)^2$$

- 3) Mean Absolute Error (MAE): MAE provided another measure of reconstruction accuracy, focusing on the absolute differences between the actual and predicted values.

$$MAE = \frac{1}{n} \sum_{i=1}^n |y_i - \hat{y}_i|$$

- 4) R-Squared (R^2): R^2 was used to quantify how well the model captured the variance in the data, with a value closer to 1 indicating better explanatory power.

$$R^2 = 1 - \frac{\sum_{i=1}^n (y_i - \hat{y}_i)^2}{\sum_{i=1}^n (y_i - \bar{y})^2}$$

where, \bar{y} is the mean of the actual values.

- 5) Variance: Variance was used to measure the spread of the prediction errors, denoted by Var . It indicates the degree to which the predicted values differ from the mean of the actual values. Lower variance suggests more consistent model predictions.

$$Var = \frac{1}{n} \sum_{i=1}^n (y_i - \bar{y})^2$$

- 6) Explained Variance Score (EVS): EVS was calculated to assess the proportion of variance explained by the model and the model's overall effectiveness.

$$EVS = 1 - \frac{Var(y_i - \hat{y}_i)}{Var(y_i)}$$

3.3.4. Decision-making framework

1) MPC: The MPC (model predictive control) framework is designed to ensure trajectory tracking a set of waypoints, with intermediate positions interpolated to generate a smooth trajectory. The prediction horizon is set to $N = 15$ steps, with sampling time (dt) set to 0.1s. The vessel's dynamics are modelled using the 3 degrees of freedom model, shown by Equations (11) and (12). The equations governing the vessel's motion are discretised using the fourth-order Runge-Kutta method during the simulation. The continuous-time state-space representation is given by the following equations:

$$\dot{\eta} = R(\psi(t))v(t) \quad (11)$$

$$M\dot{v}(t) + C(v(t))v(t) + D(v(t))v(t) = \tau(t) \quad (12)$$

where $\eta = [x, y, \psi]^T$ represents the position and heading of the vessel, $v = [u, v, r]^T$ denotes the velocities in surge, sway, and yaw, and $\tau = [\tau_x, \tau_y, N]^T$ corresponds to the control inputs (forces and moment).

The rotation matrix $R(\psi(t))$ that transforms velocities from the body-fixed frame to the inertial frame is expressed by Equation (13). Additionally, the state-output relationship is defined by the output Equation (14).

$$R(\psi(t)) = \begin{bmatrix} \cos(\psi(t)) & -\sin(\psi(t)) & 0 \\ \sin(\psi(t)) & \cos(\psi(t)) & 0 \\ 0 & 0 & 1 \end{bmatrix} \quad (13)$$

$$y(t) = C \bullet [\eta(t)^T, v(t)^T]^T; C = \begin{bmatrix} 1 & 0 & 0 & 0 & 0 & 0 \\ 0 & 1 & 0 & 0 & 0 & 0 \end{bmatrix} \quad (14)$$

In this framework, the MPC optimisation problem seeks to minimise the cost function J , presented by Equation (15), penalising deviations from the interpolated reference trajectory and the magnitude of control inputs.

$$J = \sum_{n=1}^N \left((y(k+n) - y_{ref}(k+n))^T Q (y(k+n) - y_{ref}(k+n)) \right) + \sum_{n=0}^{N-1} u(k+n)^T R u(k+n) \quad (15)$$

$$Q = \begin{bmatrix} 100 & 0 \\ 0 & 100 \end{bmatrix}, R = \begin{bmatrix} 1 & 0 \\ 0 & 1 \end{bmatrix} \quad (16)$$

where $y_{ref}(k+n)$ represents the interpolated reference trajectory at future time steps, $u(k+n)$ represents the magnitude of control inputs, and Q and R are weighting matrices, see Equation (16). These matrices prioritise minimising the tracking error while keeping the control inputs within practical limits.

2) KM-DWA: the KM-DWA algorithm uses a set of the same weights as the setting in (Song et al., 2024) to balance different objectives during navigation, including obstacle avoidance, path keeping, heading stability, etc. The DCPA and TCPA thresholds are set at 50 m and 20 s to trigger evasive actions when necessary.

4. Experiment

4.1. Dataset preparation and simulation setting

The dataset used in this study is derived from Dutch maritime traffic data within the Rotterdam port area, covering the period from 00:00 UTC on October 1, 2023 to 00:00 UTC on October 15, 2023. The data

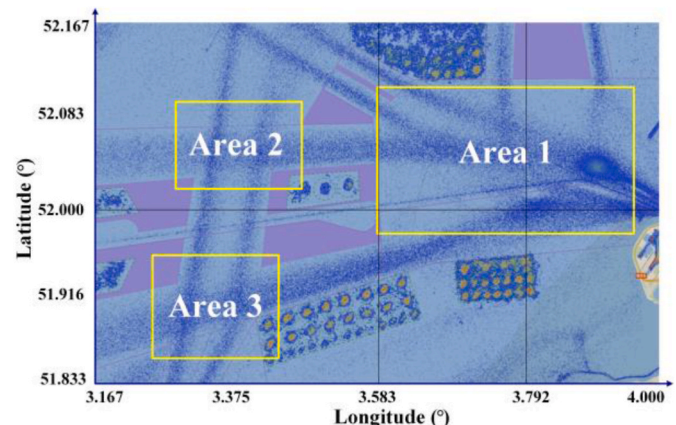


Fig. 4. The focused areas in the port of Rotterdam in the experiment.

was collected through VesselFinder and includes detailed vessel movement information within the geographical coordinates of 51.833°–52.167° latitude and 3.167°–4° longitude. This dataset specifically focuses on three high-risk areas within the Rotterdam port region, selected for their higher potential for navigational conflicts, as illustrated in Fig. 4.

Through the conflict pairs extraction algorithm, Algorithm 1, proposed in Section 3.1.2, we identified and extracted 1587 potential conflict pair sequences from the original dataset. These sequences were subsequently used for preference extraction and trajectory prediction model training and validation. During the preprocessing phase, numerical features were normalised and categorical features were encoded to ensure consistency and facilitate their utilisation by the models.

Specifically, the preference extraction was conducted on the entire dataset, using the LSTM-Autoencoder for feature compression and clustering to identify the full spectrum of the navigational preferences. Furthermore, to ensure the generalisability of the trajectory prediction model, the data was divided into a training set and a test set using an 80/20 split. In this case, 1,269 conflict pairs were allocated for training, while the remaining 318 conflict pairs were reserved for further testing and validation.

A simulation was implemented in Area 1 of Rotterdam Port to validate the proposed decision-making framework. The goal of the simulation was to evaluate the ability of a tugboat to navigate safely along predetermined routes while avoiding collisions with neighbouring vessels. For this purpose, we utilised *Tito-Neri*, a 1:30 scale model of a tugboat developed by TU Delft (Haseltalab et al., 2020). The parameters of *Tito-Neri* are provided in Table 2. These parameters can be converted according to Froude scaling of various physical quantities (Moreira et al., 2007).

In this experiment, we selected a navigational scenario from real AIS data where the own ship acts as the stand-on vessel, while the neighbouring vessel is the give-way vessel. Fig. 5 presents not only the predicted and actual trajectories for both the own and the neighbouring ships on the left side but also DCPA and TCPA variation during this interaction on the right side. In this case, the own ship (represented by red and blue markers) acts as the stand-on vessel, while the neighbouring ship (represented by green and cyan markers) is the give-way vessel. The predicted trajectories for the own ship and neighbouring ship are shown in blue and purple, respectively. Additionally, the variation of motion characteristics, including SOG, COG, DCPA and TCPA, are given in the right panel. As shown in Fig. 5. DCPA decreases as the vessels approach each other, reaching their lowest point near zero before increasing as they move apart. The TCPA similarly decreases, hitting zero at the closest point of approach, and becomes negative as the vessels begin to separate. This situation requires the own ship to be vigilant for imminent evasive actions.

4.1.1. Preference extraction

The performance of the LSTM-autoencoder model was evaluated by several key metrics: the RMSE of 0.048 and the MAE of 0.0284, indicating a high degree of accuracy in the model’s reconstruction capabilities. Additionally, the model achieved an R^2 value of 0.936 and an EVS of 0.936, reflecting its effectiveness in capturing the underlying variance in the data.

Table 2
The parameters of the *Tito-Neri* ship model.

Quantity	Length	Width	Thrustor forces	Mass	Actuators
	0.97 m	0.30 m	$\tau_x = [-5, 5]$, (N) $\tau_y = [-5, 5]$, (N) $N = [-2.5, 2.5]$ (N·m)	16.9 kg	1) Two stern azimuth thrusters 2) One bow thruster

Furthermore, we applied K-means to the encoded data produced by the LSTM-autoencoder model to identify the optimal number of clusters with identified manoeuvring preferences. The evaluation was based on three key metrics: Sum of Squared Errors (SSE), Silhouette Score, and Davies-Bouldin Index, as illustrated in Fig. 6. The selection of 4 clusters reflects a balanced consideration of these metrics. While the SSE curve shows diminishing improvements beyond 4 clusters, suggesting limited benefits from additional clusters. Additionally, although the Silhouette Score does not reach its maximum at 4 clusters, it remains relatively high, indicating a balance between intra-cluster cohesion and inter-cluster separation. Furthermore, while the lowest value of the Davies-Bouldin Index occurs at 2, the index at 4 clusters is relatively low compared to other numbers, further supporting this as the most effective configuration.

Based on this cluster selection, Figs. 7 and 8 illustrate the results of our collision avoidance experiment in port water areas, showing vessel interaction trends across the four identified manoeuvring preferences. Each trend represents specific behaviours in terms of the features of navigational preferences, including SOG, ACC, ROT, and other variables. The four clusters represent distinct vessel interaction preferences, summarised in Table 3.

Each cluster represents a different manoeuvring pattern in collision avoidance: **Cluster 0** exhibits a cautious and stable interaction pattern, where vessels maintain low speeds and straight courses with minimal adjustments. **Cluster 1** reflects a proactive strategy of accelerating through encounter points, with vessels making significant speed and course adjustments near the encounter, indicating a preference for rapid passage through potential collision areas. **Cluster 2** represents a gradual adjustment strategy, with slow changes in speed and heading, indicating a preference for steady navigation in low-risk scenarios. **Cluster 3** demonstrates a response to potentially hazardous situations, with vessels significantly increasing speed and making large course adjustments near the encounter point, suggesting a reactive strategy to avoid imminent collisions.

4.1.2. Trajectory prediction results

4.1.2.1. (1) Preference prediction. An LSTM classifier was trained and evaluated to predict navigational preferences. As shown in Fig. 9, the model achieved strong performance on the training set, with accuracy at 0.9179, precision at 0.9163, recall at 0.9179, and an F1 score of 0.9165. The slightly lower validation metrics—accuracy of 0.8460, precision of 0.8614, recall of 0.8460, and an F1 score of 0.8498—indicate minor overfitting. Nevertheless, the model demonstrates reasonable generalisation capability, which forms a solid foundation for subsequent trajectory prediction tasks.

4.1.2.2. Trajectory prediction. The proposed movement predictor, utilising the MTL-Seq2Seq-LSTM-Att model, was designed to integrate the results of preference prediction into the trajectory prediction process. Fig. 10 shows the training and validation loss curves for the trajectory prediction model over three prediction horizons: 10 min, 15 min, and 20 min. The validation loss follows a similar trend, stabilizing slightly above the training loss, which suggests good generalisation. In terms of runtime performance, the module completed each trajectory prediction in an average of 12.8 ms, meeting real-time requirements in dynamic collision avoidance scenarios.

4.1.2.3. (3) Comparative performance analysis. We compared the performance of the proposed predictive model with the following baseline methods over different forecasting horizons (10min, 15min, and 20min): (1) Basic Seq2Seq RNN (2) Basic Seq2seq attention LSTM (3) Basic Seq2Seq LSTM (4) Bi-LSTM, see Table 4 for details. These baseline models were selected because they represent different levels of complexity commonly used in sequence-to-sequence prediction. The

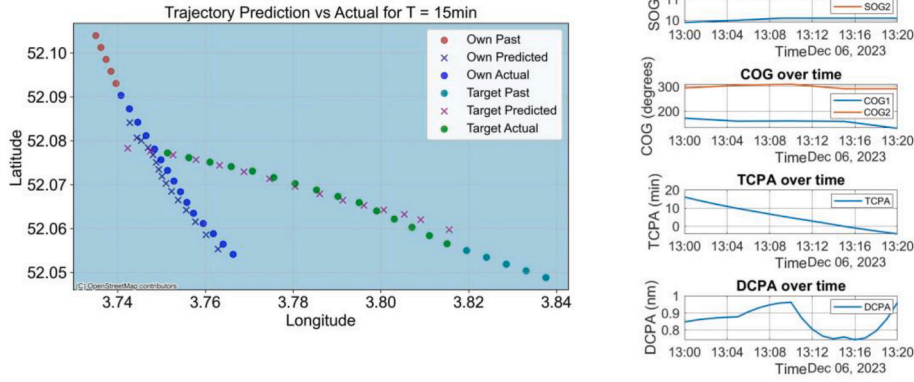


Fig. 5. Trajectory prediction vs actual trajectory for ships in a crossing scenario.

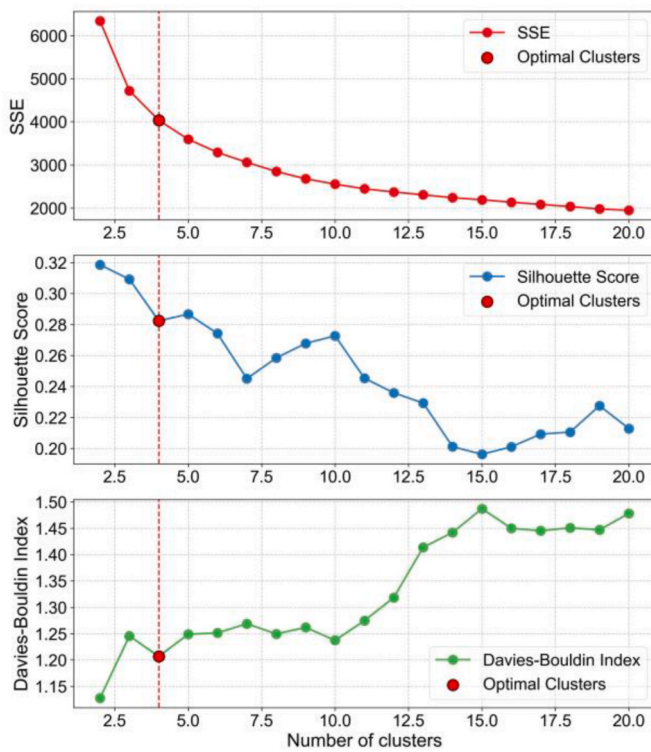


Fig. 6. The illustration of optimal clustering number investigation.

Basic Seq2Seq RNN serves as a basic model for comparison, while the Basic Seq2Seq LSTM improve upon it by handling long-term dependencies, and the Basic Seq2seq attention LSTM and the Bi-LSTM further enhance the ability to focus on important parts of the sequence or process data in both directions. The metrics used include MSE, MAE, R^2 , variance, evaluating the models' ability to predict future trajectories of the own ship and a neighbouring ship based on initial 5-min trajectory data.

- 1) **10-Minute Forecasting Horizon:** The Basic Seq2Seq LSTM model shows the lowest MSE (0.0002) and MAE (0.0097), indicating slightly better short-term prediction accuracy. However, the proposed MTL-Seq2Seq-LSTM-Att model also demonstrates acceptable performance with an MSE of 0.0003 and a high R^2 of 99.2%, comparable to the best-performing models.
- 2) **15-Minute Forecasting Horizon:** Extending the horizon to 15 min, the proposed model continues to perform competitively with an MSE

of 0.0036 and an R^2 of 89.4%. These results suggest that the model retains a good balance between accuracy and variance explanation. Although the Bi-LSTM model exhibits a lower MAE, the proposed model maintains robust overall performance. Notably, the Basic Seq2seq LSTM with Attention and without attention models show a reduction in R^2 to 86.7% and 86.19%, respectively, along with higher MSEs and MAEs, indicating a decrease in predictive accuracy over longer horizons.

- 3) **20-Minute Forecasting Horizon:** For the 20-min horizon, the performance of the models diverges more noticeably. The proposed model achieves the lowest MSE of 0.0060 and a relatively high R^2 of 85.2%, suggesting it remains effective for longer-term predictions compared to other models.

The proposed MTL-Seq2Seq-LSTM-Att model demonstrates consistent performance across different prediction horizons. While some baseline models exhibit strengths in specific metrics at certain horizons, the proposed model provides a reliable balance between accuracy and variance explanation, particularly in long-term prediction scenarios.

4.1.2.4. (4) *Visual analysis of prediction results.* The prediction results are further visualised in Figs. 13–15 in Appendix, showcasing the model's performance over 10-min, 15-min, and 20-min horizons, respectively.

For the 10-min horizon, the model generally captures the trajectory trends but exhibits deviations in certain cases, such as case 3 and case 4, indicating difficulties in handling short-term dynamics. In contrast, the 15-min horizon provides the most accurate predictions, with a close alignment between predicted and actual trajectories, demonstrating the model's ability to balance global trends with local details. At the 20-min horizon, while overall trends are still captured, slight distortions and deviations appear, particularly in more complex scenarios, reflecting a decrease in prediction precision as the forecast period extends.

The visualisation results suggest that the model performs best at the 15-min horizon, where it achieves an optimal balance between accuracy and stability. The 10-min predictions, though capturing general trends, reveal shortages in capturing fine-grained and foreseeable predictions. The 20-min horizon, on the other hand, shows the model's reduced precision over longer periods, likely due to increased uncertainty and cumulative errors. Overall, the 15-min horizon is the most suitable for practical decision-making, balancing immediate accuracy and longer-term trend stability.

4.2. Decision-making results

To anticipate the future positions of the vessels involved in the scenario, we employed the developed movement predictor in the decision-

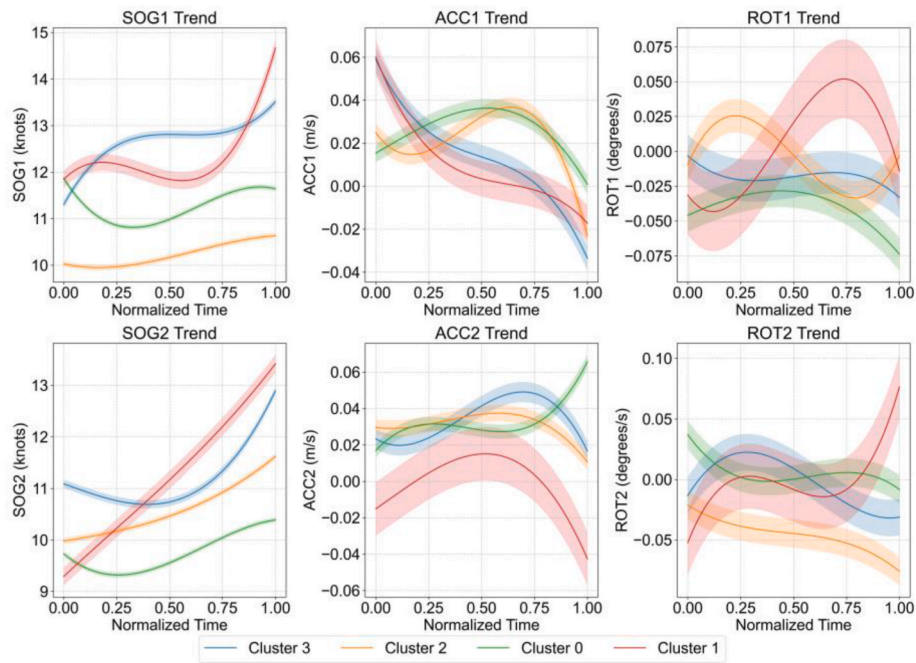


Fig. 7. Experiment of MASS in port water areas.

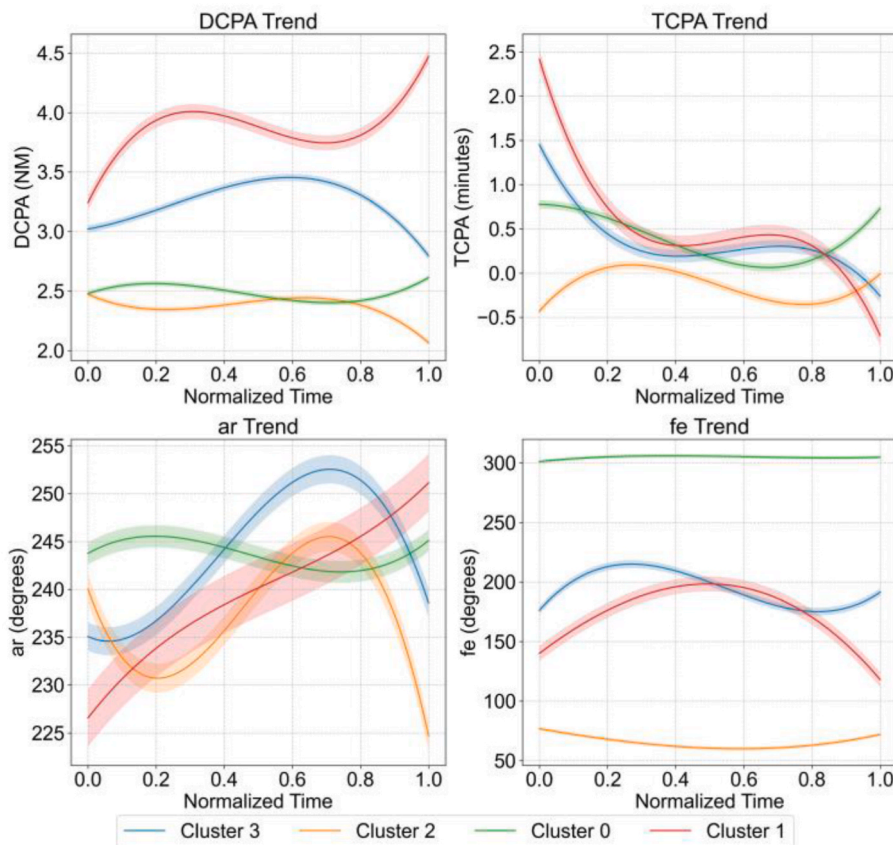


Fig. 8. Experiment of MASS in port water areas.

making framework, shown in Fig. 3. This model leverages historical 5-min AIS data to forecast the future paths of the vessels over the selected horizon of 15 min. By predicting the future trajectories, we could determine the optimal waypoints for safe navigation of the own ship. Based on the predicted trajectories, we established a series of

turning points that the vessel should follow to avoid collisions based on human-preference-aware paths. These turning points were then fed into the MPC framework, which was tasked with tracking the desired trajectory while performing local collision avoidance. The MPC was configured to optimise the vessel’s control inputs, ensuring that it

Table 3
Characteristics of the four identified vessel interaction preferences.

Cluster	0	1	2	3
SOG1	Slight decrease followed by a recovery to its initial level, with relatively low speed throughout the interaction.	Stabilise in the first half, followed by acceleration, with a slightly wider confidence interval in the first half.	The lowest overall speed, with a slight upward trend during the interaction.	Steadily increases, with a faster initial rise followed by a period of stability, then a slower ascent toward the end.
SOG2	Initially slightly decreases, then steadily accelerates.	Shows a continuous increase in speed, with a wider confidence interval.	Slow and steady acceleration, maintaining a relatively low speed.	Initially decreases slightly, remains stable, then accelerates toward the end.
ACC1	A high acceleration initially, followed by a decline.	Gradually decreases, remaining mostly in the acceleration phase, with the highest initial acceleration and the widest confidence interval early on.	Mostly in the acceleration phase, with a slight decrease followed by an increase, ending with a decline into negative acceleration.	Shows a consistent downward trend from positive to negative acceleration, with a wider confidence interval in the middle phase.
ACC2	Gradually increases, with a stable middle section.	Increases initially, then decreases, with a wide confidence interval.	Relatively stable, remaining in the positive acceleration zone, indicating consistent acceleration.	Initially increases slowly, then decreases toward the end, showing a gradual transition from acceleration to deceleration.
ROT1	The overall trend indicates a left turn, with a wide confidence interval, suggesting variability in the turning behaviour.	Starts with a slight left turn, then shifts to a right turn, with the turning rate decreasing but remaining positive and the widest confidence interval across all clusters.	Initially increases, then decreases, followed by a slow rise back to 0, indicating a fluctuating turning behaviour.	Maintains a slightly negative rate (indicating a slow left turn), with a wider confidence interval.
ROT2	Displays a minor right turn, initially decreasing and then stabilizing at 0, with a wide confidence interval.	A continuous right turn, with a stable mid-section near 0, followed by further increase; the confidence interval is the widest.	Declines steadily into negative values, indicating a consistent left turn, with a large confidence interval suggesting variability.	Increases initially, then declines below 0 and stabilises, indicating a right turn followed by a left turn, with significant variability.
DCPA	Remains stable around 2.5 nm.	Increases initially, then decreases slightly before increasing again, with the largest overall DCPA among the clusters.	Remains stable at around 2.5 nm, then decreases slightly toward the end.	Initially increases by about 0.5 nm, then decreases to approximately 2.8 nm, indicating an overall larger

Table 3 (continued)

Cluster	0	1	2	3
TCPA	Decreases gradually toward 0 and then increases.	Decreases to about 0.5 min, stabilises, and then decreases further below 0, showing the ships passing the closest point.	Mostly negative, exhibiting fluctuations, suggesting consistent proximity during the interaction.	DCPA but lower than Cluster 1. Decreases to about 0.2 min, stabilises, then decreases below 0, similar to Cluster 1.
ϕ	Maintains a stable encounter angle of around 245°.	Maintains a steady increase with a large range of variability.	Exhibits fluctuations, initially decreasing, then increasing, and decreasing again.	Displays significant fluctuations, initially increasing and then decreasing.
α	Remains stable at approximately 300°.	Rises and then returns to the initial level.	Remains stable and at the lowest value among all clusters.	Shows minor fluctuations, with a slight initial rise followed by a steady decline.

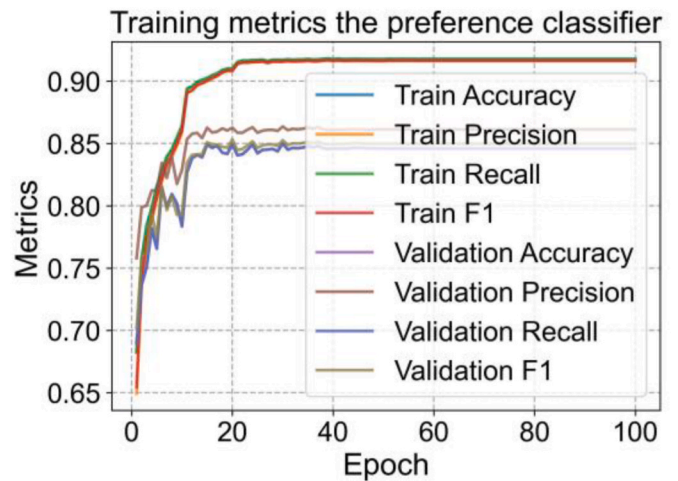


Fig. 9. Training metrics of the preference prediction classifier.

adhered to the reference path while dynamically adjusting to any emerging threats.

While in many studies – including our previous work (Song et al., 2024) - it is assumed that neighbouring vessels maintain their speed or course during interactions, this study focuses on validating the proposed predictive model in a situation where the own ship’s trajectory tracking is performed based on the future trajectory points of both the own ship and the neighbouring vessels, as predicted by our model. Moreover, we also address situations where the predicted trajectory of the neighbouring vessel poses a collision risk to the own ship. In such cases, we validated the intervention of the KM-DWA local planner to facilitate decision-making throughout the collision avoidance process. This approach was integral in demonstrating the effectiveness of our proposed model in handling dynamic maritime scenarios involving potential collision risks.

The simulation results are illustrated in Figs. 11 and 12, where the blue arrows indicate the moving direction of the own vessel, while the yellow arrows indicate the moving direction of the neighbouring vessel. Fig. 11 illustrates the path-tracking results without the local KM-DWA

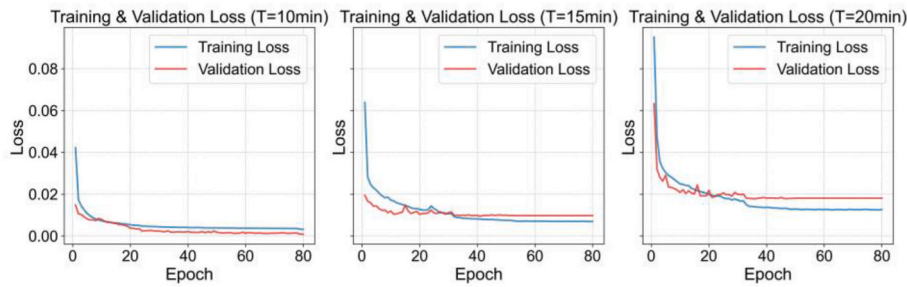


Fig. 10. Training loss of the MTL-Seq2Seq-LSTM-Att model for prediction of future length.

Table 4

The prediction results of the proposed method and other baseline predictive methods.

T	Metrics	Predictive models				
		MTL-Seq2Seq-LSTM-Att	Basic Seq 2 Seq RNN	Basic Seq2seq attention LSTM	Basic Seq2Seq LSTM	Bi-LSTM
10min	MSE	0.0003	0.0003	0.0004	0.0002	0.0005
	MAE	0.0113	0.0106	0.0129	0.0097	0.0156
	R ²	99.2%	99.2%	98.6%	99.2%	98.5%
	var	0.0003	0.0003	0.0004	0.0002	0.0005
15min	MSE	0.0036	0.0042	0.0046	0.0048	0.0039
	MAE	0.0389	0.0414	0.0435	0.0408	0.0381
	R ²	89.4%	87.8%	86.7%	86.19%	88.7%
	var	0.0036	0.0042	0.0045	0.0048	0.0039
20min	MSE	0.0060	0.0117	0.0105	0.0103	0.0100
	MAE	0.0488	0.0754	0.0612	0.0564	0.0566
	R ²	85.2%	71.0%	74.23%	74.5%	75.4%
	var	0.0060	0.0116	0.0102	0.0102	0.0098

intervention, while Fig. 12 shows the path-tracking results with KM-DWA intervention. In the left panel of the two figures, the reference path is depicted as a red dashed line, the path generated by the MPC controller is represented as a solid blue line, and the yellow line illustrates the predicted trajectory of the neighbouring vessel. A close alignment between the reference path and the MPC tracking path demonstrates effective path-following control, ensuring the vessel adheres closely to the desired trajectory. The right panel presents the ship motion parameters during the avoidance process, such as speed, heading, and relative motion characteristics between the vessels, with a focus on DCPA and TCPA. The own vessel maintains stability by controlling the surge speed throughout the tracking process. Meanwhile, the sway

and yaw speeds remain near zero as the ship adjusts its heading to follow the desired trajectory. The observed trend of DCPA initially decreasing and then increasing, along with TCPA continuously decreasing, reflects the scenario where the two vessels approached each other before reaching the closest point of approach and subsequently diverged in opposite directions.

Fig. 12 presents the path-tracking results where the knowledge maps-based DWA path planner is applied. In this case, the DWA was triggered upon the DCPA and TCPA values reaching the set thresholds of 50 m and 20 s, respectively. As shown in the blue tracking path in the left panel, the vessel makes an early right turn at $t = 61$ s in response to the detected risk. This manoeuvre, reflected in changes to sway and yaw speeds, adjusts the COG1 and gradually increases the DCPA. As shown in the right panel, the minimum DCPA improves from 21.59 to 24.67 after intervention, indicating a safer distance between the vessels.

The results from these simulations underscore the importance of the proposed decision-making framework for autonomous vessel navigation. While the MPC is capable of tracking the reference path well, the inclusion of KM-DWA enhances the safety of the navigation by responding dynamically to emerging collision risks by taking account of the ship's manoeuvrability. This approach underscores the potential of combining MPC and KM-DWA to ensure precise path following, collision avoidance, and operational efficiency in real-world maritime navigation.

5. Discussion

This study aimed to develop a human-preferences-aware trajectory prediction model, which serves as the foundation for a decision-making framework aimed at enabling autonomous vessels to perform human-mimic navigation during collision avoidance in a mixed waterborne environment. The results demonstrated that the proposed framework successfully extracted navigational preferences from AIS data, predicted

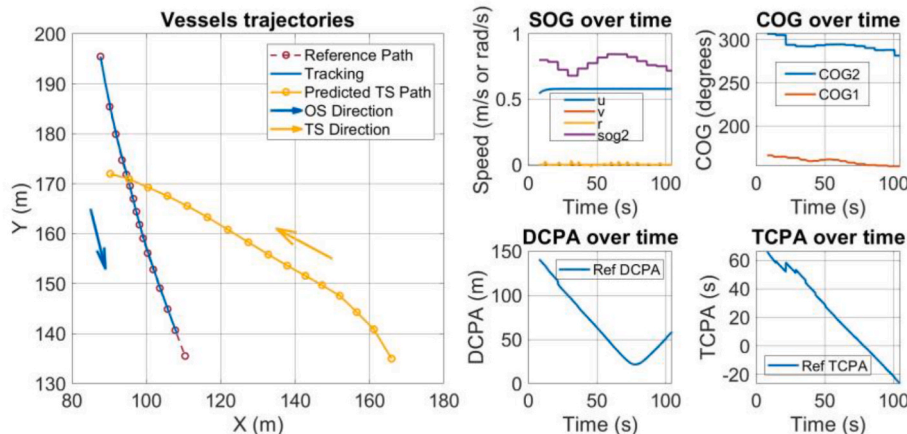


Fig. 11. Demonstration of path tracking based on predictive trajectory results.

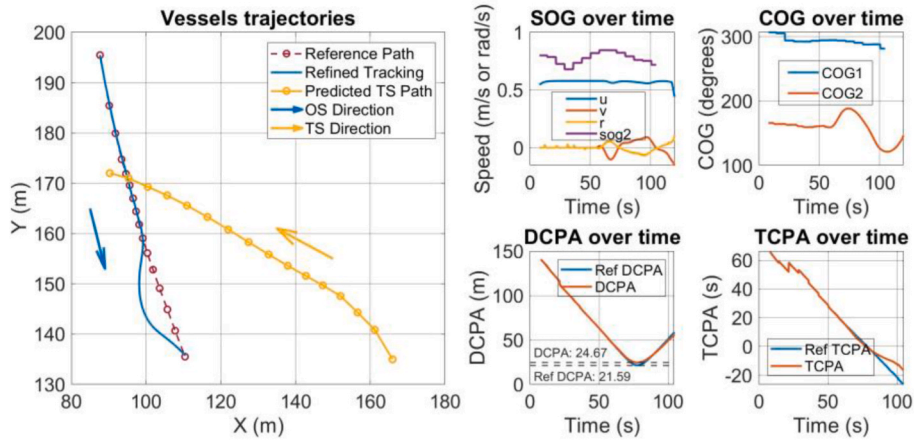


Fig. 12. Demonstration of path tracking based on refined path results.

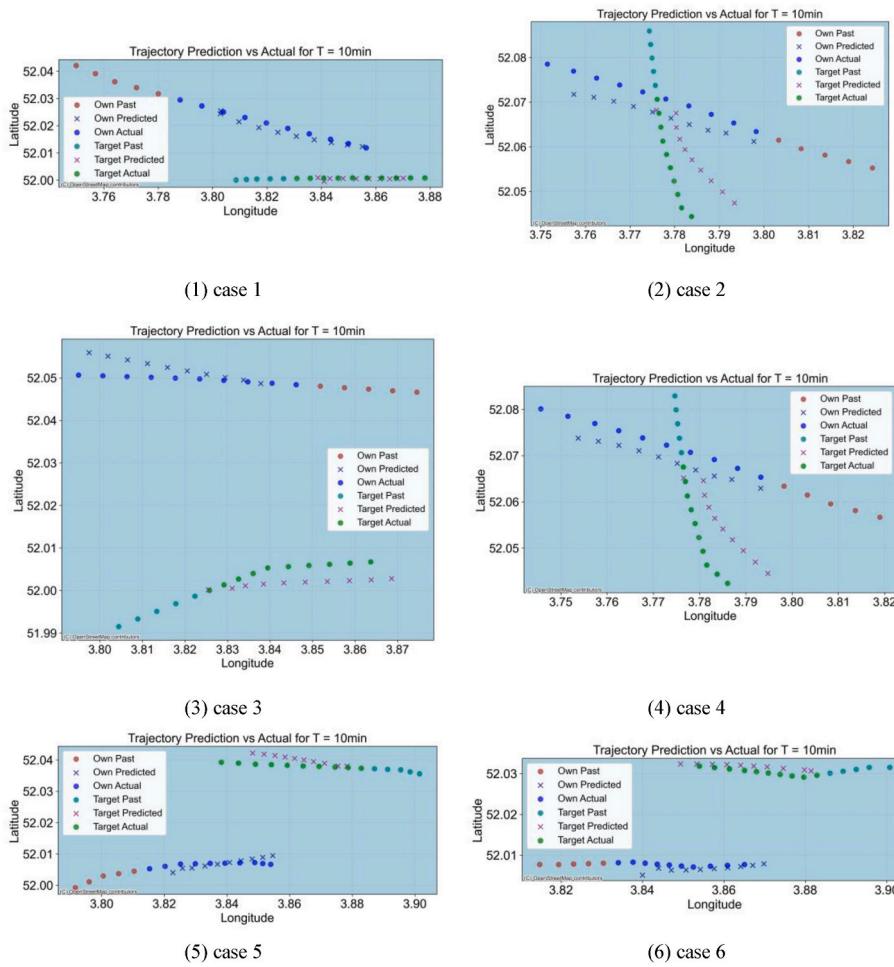


Fig. 13. The visualisation results for the prediction horizon of 10min.

future trajectories with high accuracy, and enhanced collision avoidance strategies by incorporating these predictions into the decision-making process.

5.1. Interpretation of results

The extraction of navigational preferences using the LSTM-autoencoder and K-means clustering revealed four distinct clusters representing different manoeuvring patterns during vessel encounters.

Each cluster provided insights into how vessels adjust their speed, acceleration, and rate of turn in response to potential collision scenarios. For instance, Cluster 0 reflected a cautious and stable interaction pattern, while Cluster 3 demonstrated a more reactive strategy involving significant course adjustments and speed variations. These human preference patterns were critical in improving the accuracy and interpretability of the trajectory predictions, allowing the MTL-Seq2Seq-LSTM-Att model to capture the dynamic interactions between vessels more effectively. Additionally, with an average prediction time of 12.8

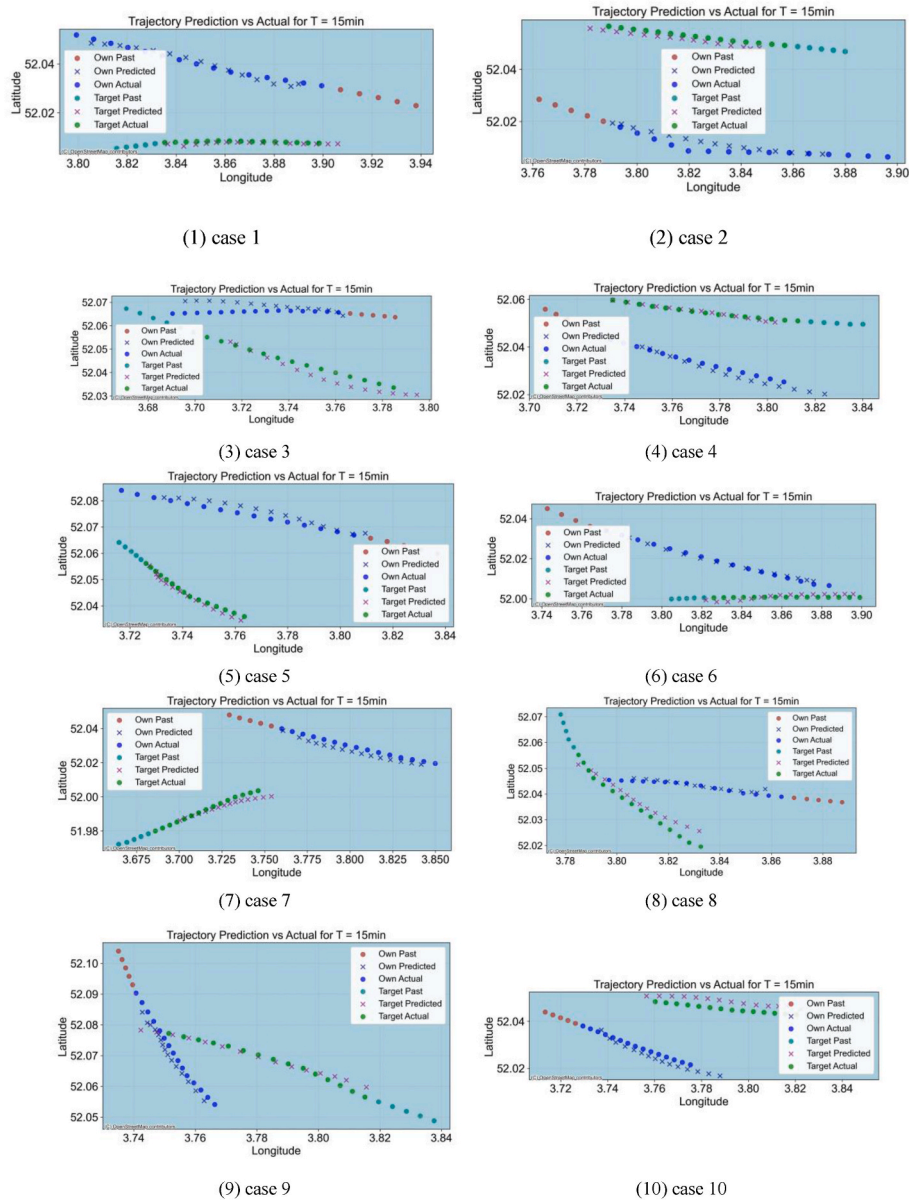


Fig. 14. The visualisation results for the prediction horizon of 15min.

ms on a standard computation platform, the module ensures the real-time requirement for collision avoidance.

The predictive performance of the trajectory prediction model is related to the roles of its components. The encoder captures temporal dependencies by transforming historical trajectory data into latent representations, which preserve critical information for accurate predictions. The decoder integrates navigational preferences to generate future trajectories that align with specific manoeuvring patterns, while the attention mechanism dynamically weighs input features to focus on relevant aspects of vessel interactions. These components collectively contribute to reducing prediction errors and exhibit good performance across various time horizons, particularly at the 15-min horizon. The model effectively balanced global trend capture with local detail fidelity, demonstrating that the inclusion of human navigational preferences enhances the credibility and accuracy of trajectory predictions. This improved accuracy is crucial for the subsequent decision-making processes, where these predictions inform both the own ship's and the neighbouring ship's future paths.

The extension of the decision-making framework with the predicted trajectories allowed for more context-aware navigation. Unlike previous

approaches, which assumed constant speed and course for neighbouring vessels, this study leveraged the trajectory prediction model to proactively anticipate and react to potential collision risks. By integrating real-time human-preference-aware predictions into the decision-making framework, the framework facilitated avoidance manoeuvres and enabled local path-planning adjustments based on real-time DCPA and TCPA evaluations. This dual approach ensures that both navigational preferences and safety considerations are addressed.

The primary innovation lies in the predictor model, which integrates navigational preferences extracted from AIS data to predict future trajectories. The decision-making framework, designed around this prediction model, incorporates the KM-DWA module for local path refinement and the MPC module for trajectory tracking. The integration demonstrates the feasibility of combining human-preference-aware trajectory predictions with established decision-making methods, serving as the practical foundation for achieving human-mimic navigation during the interactive collision avoidance process in a mixed waterborne environment.

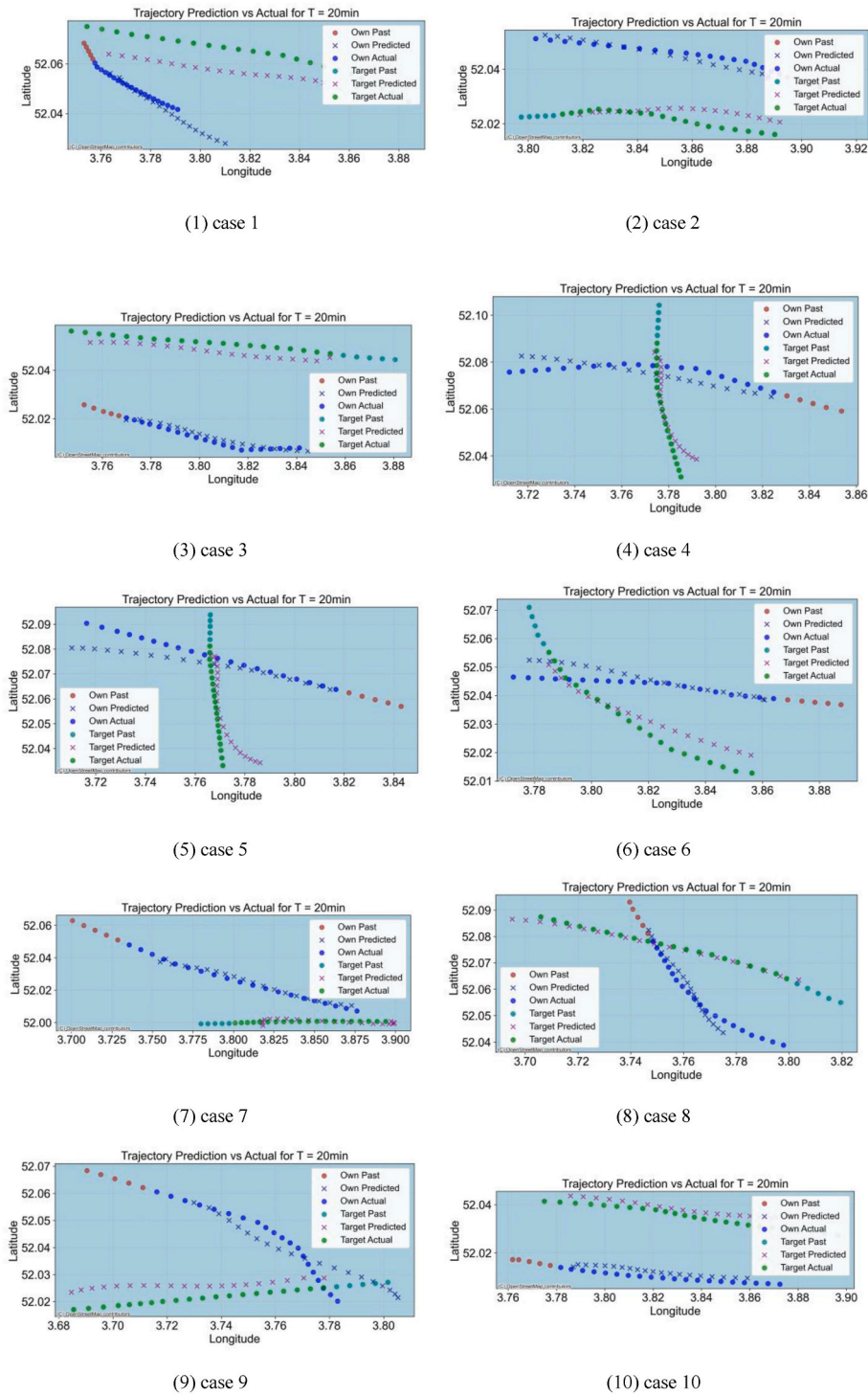


Fig. 15. The visualisation results for the prediction horizon of 20min.

5.2. Practical implications

By providing a more accurate prediction of both the own ship's and the neighbouring vessel's trajectories, the framework supports safer and more human-friendly navigation in mixed waterborne environments. This approach allows for more proactive collision avoidance strategies that account for the movement of surrounding vessels rather than relying on static assumptions.

Furthermore, maintaining mutual trust between autonomous vessels and human-operated ships becomes critical in environments where

direct communication between vessels is limited or nonexistent. This study acknowledges that autonomous ships while making independent navigational decisions, must also act in predictable and trustworthy ways to human operators—both those on neighbouring vessels and those supervising the autonomous ships. By adhering to predictable navigational patterns and demonstrating an understanding of navigational preferences, autonomous vessels can foster trust (Poornikoo et al., 2024), reduce uncertainty, and improve safety in mixed waterborne scenarios.

7. Conclusion

This study advances state of the art by integrating real-time trajectory predictions into a MASS decision-making framework, enabling safer and smoother interaction for collision avoidance, addressing human-preference-based manoeuvres and real-time local planning for avoiding obstacles. The methods of MPC (Zheng et al., 2014) and KM-DWA proposed by (Song et al. 2022, 2024) used in this study validated the feasibility and effectiveness of combining these approaches with a new navigational predictive model based on human preference data.

The key contributions of this research include.

1. *Human navigational preference extraction*: Developed a methodology to extract navigational preferences based on ship conflict pairs extracted from AIS data through an LSTM-autoencoder and K-means clustering.
2. *Trajectory prediction model*: Designed and validated an MTL-Seq2Seq-LSTM-Att model to predict ship trajectories considering extracted human navigational preferences for improved accuracy.
3. *Framework integration*: Proposed a decision-making framework that integrates the prediction model with established path planning and tracking methods, demonstrating the practical applicability of the prediction model in real-time collision avoidance.

Despite these promising results, several limitations are acknowledged, including the limited geographic scope and timeframe of the dataset, the focus on two-vessel interactions, the absence of environmental considerations, the increased computational complexity in high-density traffic scenarios, and the need for a better understanding of human trust dynamics. These limitations highlight the need for further research to enhance the generalisability and robustness of the framework.

Future work will pursue further refinement, testing and validation of the framework in these directions. These efforts are crucial for ensuring that autonomous maritime systems can operate safely and efficiently in complex and congested environments by remaining predictable and trustworthy, ultimately leading to broader acceptance and adoption of autonomous technologies in the maritime industry.

CRedit authorship contribution statement

Rongxin Song: Writing – original draft, Validation, Software, Methodology, Conceptualization. **Eleonora Papadimitriou**: Writing – review & editing, Supervision, Conceptualization. **Rudy R. Negenborn**: Writing – review & editing, Supervision, Resources, Conceptualization. **Pieter van Gelder**: Writing – review & editing, Supervision, Resources, Project administration, Conceptualization.

6. Limitations and future work

While the study successfully demonstrates the integration of a trajectory prediction model with established decision-making methods, several limitations must be acknowledged.

- (1) **Data limitations**: The dataset, while detailed, was limited to the Rotterdam port area and a specific timeframe. This geographic and temporal restriction may limit the generalisability of the findings to other maritime navigational environments.
- (2) **Scope of vessel interactions**: The study primarily focused on two-vessel interactions, simplifying the real-world complexity of maritime navigation where multiple vessels often interact simultaneously. While the KM-DWA provides local path refinement to ensure safety, it is designed for pairwise interactions and does not address the interactive effects of the movements of multiple vessels in congested environments. In multi-vessel scenarios, the interdependence of vessels' trajectories requires

dynamic conflict modelling, which was not explored in this work. Future research should extend the current framework to incorporate multi-vessel coordination mechanisms in collision avoidance scenarios.

- (3) **Consideration of environmental factors**: The current simulations do not consider environmental factors such as wind, waves, currents, or restricted visibility, which directly affect vessel manoeuvring and collision avoidance. Future work will include these factors to test the framework's performance in more realistic and diverse maritime conditions.
- (4) **Computational complexity**: The integration of multiple predictive and decision-making models increases the computational complexity, which may affect real-time performance in high-density traffic scenarios or when deployed on vessels with limited processing capabilities.
- (5) **Human trust dynamics**: While the framework accounts for the navigational preferences of both the own ship and the neighbouring ship, it does not fully model the dynamics of trust between human operators/supervisors and MASS. In scenarios where direct communication is limited, autonomous ships must behave in a way that earns and maintains the trust of human operators. This aspect of human-autonomous interaction is crucial for ensuring safe and coordinated manoeuvres in mixed environments.

Declaration of competing interest

The authors declare that they have no known competing financial interests or personal relationships that could have appeared to influence the work reported in this paper.

Acknowledgement

This study is the result of the research project funded by the China Scholarship Council under grant 202106950002 and supported by Researchlab Autonomous Shipping (RAS) of Delft University of Technology.

References

- Akdağ, M., Pedersen, T.A., Fossen, T.I., Johansen, T.A., 2024. A decision support system for autonomous ship trajectory planning. *Ocean Eng.* 292, 116562. <https://doi.org/10.1016/J.OCEANENG.2023.116562>.
- Alam, M.M., Spadon, G., Etemad, M., Torgo, L., Milios, E., 2024. Enhancing short-term vessel trajectory prediction with clustering for heterogeneous and multi-modal movement patterns. *Ocean Eng.* 308. <https://doi.org/10.1016/j.oceaneng.2024.118303> [Internet].
- Chen, L., Hopman, H., Negenborn, R.R., 2018. Distributed model predictive control for vessel train formations of cooperative multi-vessel systems. *Transp. Res. C Emerg. Technol.* 92, 101–118. <https://doi.org/10.1016/j.trc.2018.04.013> [Internet].
- Chen, P., Huang, Y., Mou, J., van Gelder, P.H.A.J.M., 2018. Ship collision candidate detection method: a velocity obstacle approach. *Ocean Eng.* 170, 186–198. <https://doi.org/10.1016/j.oceaneng.2018.10.023> [Internet].
- Du, L., Goerlandt, F., Kujala, P., 2020. Review and analysis of methods for assessing maritime waterway risk based on non-accident critical events detected from AIS data. *Reliab Eng Syst Saf* [Internet] 200, 106933. <https://doi.org/10.1016/j.res.2020.106933>.
- Düz, B., van Iperen, E., 2024. Ship trajectory prediction using encoder-decoder-based deep learning models. *J. Locat. Based Serv.* <https://doi.org/10.1080/17489725.2024.2306339> [Internet].
- Gan, L., Ye, B., Huang, Z., Xu, Y., Chen, Q., Shu, Y., 2023. Knowledge graph construction based on ship collision accident reports to improve maritime traffic safety. *Ocean Coast Manag.* 240, 106660. <https://doi.org/10.1016/J.OCECOAMAN.2023.106660>.
- Gao, M., Liang, M., Zhang, A., Hu, Y., Zhu, J., 2024. Multi-ship encounter situation graph structure learning for ship collision avoidance based on AIS big data with spatio-temporal edge and node attention graph convolutional networks. *Ocean Eng.* 301. <https://doi.org/10.1016/j.oceaneng.2024.117605> [Internet].
- Gil, M., 2021. A concept of critical safety area applicable for an obstacle-avoidance process for manned and autonomous ships. *Reliab Eng Syst Saf* [Internet] 214, 107806. <https://doi.org/10.1016/j.res.2021.107806>.
- Haseltalab, A., Garofano, V., Afzal, M.R., Faggioni, N., Li, S., Liu, J., Ma, F., Martelli, M., Singh, Y., Slaets, P., et al., 2020. The collaborative autonomous shipping experiment (Case): motivations, theory, infrastructure, and experimental challenges [Internet]. <https://doi.org/10.24868/issn.2631-8741.2020.014>. (Accessed 2 July 2024).

- Huang, L., Wan, C., Wen, Y., Song, R., van Gelder, P., 2024. Generation and application of maritime route networks: overview and future research directions. *IEEE Trans. Intell. Transport. Syst.* <https://doi.org/10.1109/TITS.2024.3492060>.
- Huang, L., Wen, Y., Guo, W., Zhu, X., Zhou, C., Zhang, F., Zhu, M., 2020. Mobility pattern analysis of ship trajectories based on semantic transformation and topic model. *Ocean Eng.* 201, 107092. <https://doi.org/10.1016/j.oceaneng.2020.107092> [Internet].
- Huang, Y., Chen, L., Negenborn, R.R., van Gelder, P.H.A.J.M., 2020. A ship collision avoidance system for human-machine cooperation during collision avoidance. *Ocean Engineering* [Internet] 217, 107913. <https://doi.org/10/gn7j5m>.
- Huang, Y., van Gelder, P.H.A.J.M., Wen, Y., 2018. Velocity obstacle algorithms for collision prevention at sea. *Ocean Eng.* 151, 308–321. <https://doi.org/10.1016/j.oceaneng.2018.01.001> [Internet].
- Jiang, F., Wang, H., Li, Y., 2024. VesNet: a vessel network for jointly learning route pattern and future trajectory. *ACM Trans Intell Syst Technol* [Internet] 15 (2), 1–25. <https://doi.org/10.1145/3639370>.
- Liu, K., Yuan, Z., Xin, X., Zhang, J., Wang, W., 2021. Conflict detection method based on dynamic ship domain model for visualization of collision risk Hot-Spots. *Ocean Engineering* [Internet] 242, 110143. <https://doi.org/10.1016/j.oceaneng.2021.110143>.
- Liu, R.W., Hu, K., Liang, M., Li, Y., Liu, X., Yang, D., 2023. QSD-LSTM: vessel trajectory prediction using long short-term memory with quaternion ship domain. *Applied Ocean Research* [Internet] 136. <https://doi.org/10.1016/j.apor.2023.103592>.
- Liu, R.W., Liang, M., Nie, J., Lim, W.Y.B., Zhang, Y., Guizani, M., 2022. Deep learning-powered vessel trajectory prediction for improving smart traffic services in maritime internet of things. *IEEE Trans Netw Sci Eng* [Internet] 9 (5), 3080–3094. <https://doi.org/10.1109/TNSE.2022.3140529>.
- Liu, Z., Wu, Z., Zheng, Z., 2019. A novel framework for regional collision risk identification based on AIS data. *Applied Ocean Research* [Internet] 89, 261–272. <https://doi.org/10.1016/j.apor.2019.05.020>.
- Luong, M.-T., Pham, H., Manning, C.D., 2015. Effective Approaches to Attention-Based Neural Machine Translation, pp. 17–21.
- Mehri, S., Alesheikh, A.A., Basiri, A., 2023. A context-aware approach for vessels' trajectory prediction. *Ocean Eng.* 282. <https://doi.org/10.1016/j.oceaneng.2023.114916> [Internet].
- Moreira, L., Fossen, T.I., Guedes Soares, C., 2007. Path following control system for a tanker ship model. *Ocean Eng.* 34 (14–15), 2074–2085. <https://doi.org/10.1016/J.OCEANENG.2007.02.005>.
- Moussalli, R., Srivatsa, M., Asaad, S., 2015. Fast and flexible conversion of geohash codes to and from latitude/longitude coordinates. *Proceedings - 2015 IEEE 23rd Annual International Symposium on Field-Programmable Custom Computing Machines, FCCM 2015*, pp. 179–186. <https://doi.org/10.1109/FCCM.2015.18>.
- Murray, B., Perera, L.P., 2018. A data-driven approach to vessel trajectory prediction for safe autonomous ship operations. In: 2018 Thirteenth International Conference on Digital Information Management (ICDIM), pp. 240–247. <https://doi.org/10.1109/ICDIM.2018.8847003> [place unknown].
- Murray, B., Perera, L.P., 2022. Ship behavior prediction via trajectory extraction-based clustering for maritime situation awareness. *J. Ocean Eng. Sci.* 7 (1), 1–13. <https://doi.org/10.1016/j.joes.2021.03.001> [Internet].
- Poornikoo, M., Gyldesten, W., Vesin, B., Øvergård, K.I., 2024. Trust in automation (TiA): simulation model, and empirical findings in supervisory control of maritime autonomous surface ships (MASS). *Int J Hum Comput Interact* [Internet] (2024 Sep 16), 1–28. <https://doi.org/10.1080/10447318.2024.2399439>.
- Rong, H., Teixeira, A.P., Guedes Soares, C., 2022. Ship collision avoidance behaviour recognition and analysis based on AIS data. *Ocean Eng.* 245, 110479. <https://doi.org/10.1016/j.oceaneng.2021.110479> [Internet].
- Shu, Y., Han, B., Song, L., Yan, T., Gan, L., Zhu, Y., Zheng, C., 2024. Analyzing the spatio-temporal correlation between tide and shipping behavior at estuarine port for energy-saving purposes. *Appl. Energy* 367, 123382. <https://doi.org/10.1016/J.APENERGY.2024.123382>.
- Shu, Y., Zhu, Y., Xu, F., Gan, L., Lee, P.T.W., Yin, J., Chen, J., 2023. Path planning for ships assisted by the icebreaker in ice-covered waters in the Northern Sea Route based on optimal control. *Ocean Eng.* 267, 113182. <https://doi.org/10.1016/J.OCEANENG.2022.113182>.
- Song, R., Papadimitriou, E., Negenborn, R.R., Gelder, P van, 2024. Integrating situation-aware knowledge maps and dynamic window approach for safe path planning by maritime autonomous surface ships. *Ocean Eng.* 311 (118882). <https://doi.org/10.1016/J.OCEANENG.2024.118882> [Internet]2024 Aug 7.
- Song R, Papadimitriou E, Negenborn RR, van Gelder P. Safety and efficiency of human-MASS interactions: towards an integrated framework. *Journal of Marine Engineering & Technology* [Internet].:1–20. <https://doi.org/10.1080/20464177.2024.2414959>.
- Song, R., Papadimitriou, E., Negenborn, R.R., van Gelder, P.H.A.J.M., 2022. Constructing knowledge maps for situation awareness of maritime autonomous surface ships. In: *Proceedings of the International Ship Control Systems Symposium*. <https://doi.org/10.24868/10722> [place unknown].
- Szlapczynski, R., Krata, P., 2018. Determining and visualizing safe motion parameters of a ship navigating in severe weather conditions. *Ocean Engineering* [Internet] 158, 263–274. <https://doi.org/10.1016/j.oceaneng.2018.03.092>.
- Szlapczynski, R., Krata, P., Szlapczynska, J., 2018. A ship domain-based method of determining action distances for evasive manoeuvres in stand-on situations. *J Adv Transp* [Internet] 2018, e3984962. <https://doi.org/10.1155/2018/3984962>.
- Szlapczynski, R., Szlapczynska, J., 2021. A ship domain-based model of collision risk for near-miss detection and Collision Alert Systems. *Reliab Eng Syst Saf* [Internet] 214, 107766. <https://doi.org/10.1016/j.res.2021.107766>.
- Thind, N.S., Hering, J., Söffker, D., 2022. Fast and precise generic model for position-based trajectory prediction of inland waterway vessels. *Automation* [Internet] 3 (4), 633–645. <https://doi.org/10.3390/automation3040032>.
- Wang, S., Li, Y., Xing, H., Zhang, Z., 2024. Vessel trajectory prediction based on spatio-temporal graph convolutional network for complex and crowded sea areas. *Ocean Engineering* [Internet] 298. <https://doi.org/10.1016/j.oceaneng.2024.117232>.
- Westrenen, F van, 2020. Institution MB-P of the, undefined. Improving conflicts detection in maritime traffic: Case studies on the effect of traffic complexity on ship collisions 234 (1), 209–222. <https://doi.org/10.1177/1475090219845975>, 2020 journals.sagepub.com [Internet].
- Xin, X., Liu, K., Yang, Z., Zhang, J., Wu, X., 2021. A probabilistic risk approach for the collision detection of multi-ships under spatiotemporal movement uncertainty. *Reliab Eng Syst Saf* [Internet] 215, 107772. <https://doi.org/10.1016/j.res.2021.107772>.
- Yang, C.-H., Lin, G.-C., Wu, C.-H., Liu, Y.-H., Wang, Y.-C., Chen, K.-C., 2022. Deep learning for vessel trajectory prediction using clustered AIS data. *Mathematics* 10 (16). <https://doi.org/10.3390/math10162936> [Internet].
- Zhang, J., Liu, J., Hirdaris, S., Zhang, M., Tian, W., 2023. An interpretable knowledge-based decision support method for ship collision avoidance using AIS data. *Reliab Eng Syst Saf* [Internet] 230, 108919. <https://doi.org/10.1016/j.res.2022.108919>.
- Zhang, M., Montewka, J., Manderbacka, T., Kujala, P., Hirdaris, S., 2021. A big data analytics method for the evaluation of ship - ship collision risk reflecting hydrometeorological conditions. *Reliab Eng Syst Saf* [Internet] 213, 107674. <https://doi.org/10.1016/j.res.2021.107674>.
- Zhang, W., Feng, X., Goerlandt, F., Liu, Q., 2020. Towards a Convolutional Neural Network model for classifying regional ship collision risk levels for waterway risk analysis. *Reliab Eng Syst Saf* [Internet] 204, 107127. <https://doi.org/10.1016/j.res.2020.107127>.
- Zhang, X., Liu, J., Chen, K., Gong, P., Liu, Y., Wu, Z., 2024. Learning dynamic interactions and long-term patterns with spatio-temporal graphs for multi-vessel trajectory prediction. *IEEE Transactions on Intelligent Vehicles* 1–16. <https://doi.org/10.1109/TIV.2024.3401864> [Internet].
- Zheng, H., Negenborn, R.R., Lodewijks, G., 2014. Trajectory tracking of autonomous vessels using model predictive control. *IFAC Proc. Vol.* 47 (3), 8812–8818. <https://doi.org/10.3182/20140824-6-ZA-1003.00767>.